Journal of Materials Chemistry C

Accepted Manuscript

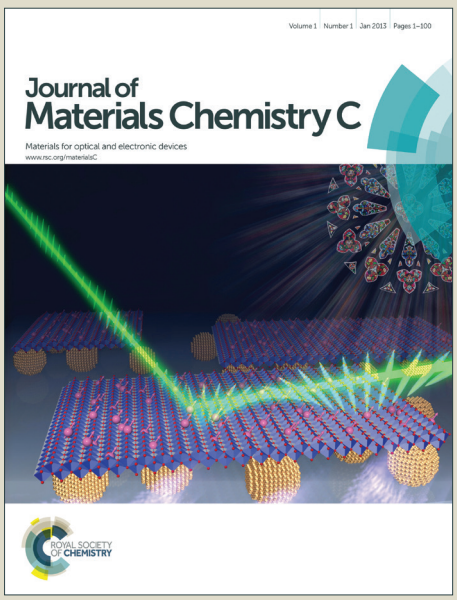

ROYAL SOCIETY OF CHEMISTRY

www.rsc.org/materialsC

Journal of
Materials Chemistry C

RSC Publishing

ARTICLE

An efficient green-emitting α-$Ca_{1.65}Sr_{0.35}SiO_4$:Eu^{2+} phosphor for UV/n-UV w-LEDs: synthesis, luminescence and thermal properties

Cite this: DOI: 10.1039/x0xx00000x

Received,
Accepted

DOI: 10.1039/x0xx00000x

www.rsc.org/

Kai Li,[ac] Ju Xu,[b] Xuechao Cai,[ac] Jian Fan,[a] Yang Zhang,[ac] Mengmeng Shang,[a] Hongzhou Lian*[a] and Jun Lin*[a]

A series of Eu^{2+} singly doped α-$Ca_{1.65}Sr_{0.35}SiO_4$:Eu^{2+} phosphors have been synthesized via the high-temperature solid-state reaction method. X-ray diffraction (XRD), Fourier transform infrared (FT-IR), scanning electron microscope (SEM), diffuse reflectance spectra and photoluminescence (PL) including temperature-dependent PL were used to characterize the as-prepared samples. The XRD patterns and Rietveld refinement of the represented sample show the pure phase for the as-prepared samples. All of the phosphors exhibit intense and broad absorption bands in the ultraviolet and near ultraviolet (n-UV) range, and produce bright green emissions upon 365 nm UV radiation. The critical concentration of Eu^{2+} for the maximum intensity was determined to be about 1mol % in α-$Ca_{1.65}Sr_{0.35}SiO_4$:Eu^{2+} after optimizing the composition. The energy transfer mechanism between Eu^{2+} was demonstrated to be dipole–dipole interaction. Besides, the fluorescence decay curves, temperature dependence PL and CIE value of α-$Ca_{1.65}Sr_{0.35}SiO_4$:Eu^{2+} phosphors were investigated. It is reasonable that the decay times of samples decrease with increasing Eu^{2+} content. The CIE chromaticity coordinates shift from green (0.197, 0.395) to the border between green and yellow (0.242, 0.547) region, which agree with the corresponding emission spectra. The maximum quantum yield is 69% for α-$Ca_{1.65}Sr_{0.345}SiO_4$:0.005Eu^{2+}. The thermal stability of luminescence of selected α-$Ca_{1.65}Sr_{0.34}SiO_4$:0.01Eu^{2+} was also investigated and compared with that of the commercial green phosphor, which shows its good performance. The above results suggest it a good candidate for green-emitting phosphors applied in UV/n-UV pumped w-LEDs.

1. Introduction

Phosphor conversion white light-emitting diodes (w-LEDs), a technology for next generation solid-state lighting systems instead of current traditional fluorescent and incandescent lamps, have attracted considerable attention due to their unique merits such as long operational lifetime, high efficiency, low thermal radiation, compactness, low energy consumption besides environmental friendliness.[1] Currently, most fabricated w-LEDs are based on the employment of a blue LED chip and yellow phosphor $Y_3Al_5O_{12}$:Ce (YAG:Ce). However, there exist the problems of the low color rendering index (CRI<80) and the high correlated color temperature (CCT) of 7765 K[2] owing to the deficiency of a red component in the emission spectrum, which limit their use in more vivid applications. Therefore, UV/n-UV LED chips coated with tricolour (blue/green/red) phosphors were devolved to obtain warm white light with high color uniformity and CRI, which can be expected to occupy the market in the near future.[3] In view of this, the attentions and interests focused on new phosphors excited by the UV/n-UV radiation are constantly increasing, which makes it a hot research topic in the phosphors field. Consequently, designing different tricolor phosphors is of great importance to meet the forthcoming demand in the fabrication process of w-LED. It is well known that the Eu^{2+} ion is sensitive to the crystal field and covalence since its 4f-5d transition is spin-allowed, which generally presents superior absorption bands in the spectral region of 250-450 nm,[4] matching well with the UV and n-UV LED chips, and broad emission spectra from blue to red region in Eu^{2+} doped phosphors. Many investigations have been devoted to them such as $Na_3(Y,Sc)Si_3O_9$:Eu^{2+}, $Li_2Ca_2Si_2O_7$:Eu^{2+}, $Na_xCa_{1-x}Al_{2-x}Si_{2+x}O_8$:$Eu^{2+}$ (x = 0.34), $Sr_{2-x}Si_5N_8$:Eu_x, $Ca_{1.5}Ba_{0.5}Si_5N_6O_3$:$Eu^{2+}$.[5]

[a]*State Key Laboratory of Rare Earth Resource Utilization, Changchun Institute of Applied Chemistry, Chinese Academy of Sciences (CAS), Changchun 130022 (P. R., China.). Email: jlin@ciac.ac.cn; hzlian@ciac.ac.cn. Fax: +86-431-85698041; Tel: +86-431-85262031*
[b]*State Key Laboratory of Structural Chemistry, Fujian Institute of Research on the Structure of Matter, CAS, Fuzhou, Fujian 350002, PR China*
[c]*University of Chinese Academy of Sciences, Beijing 100049 (P. R., China.)*

At present, as is known to us, studies on alkaline-earth silicate materials which are abundant with many kinds of crystal structures and therefore can be as the hosts for doping rare earth elements to obtain various phosphors. They possess many alluring features such as mechanical, good thermal, chemical and physical stabilities owing to their strong and rigid frameworks with covalent Si-O bonds,[6] which may make them be usefully utilized as the hosts for doping rare earth ions in the field of solid-state lighting, such as $Ba_3MgSi_2O_8:Eu^{2+}$, Mn^{2+}, $CaMgSi_2O_6:Eu^{2+}$, Mn^{2+}, $Ca_3Si_2O_7:Eu^{2+}$, $Sr/Ca_2MgSi_2O_7:Eu^{2+}$, Dy^{3+}.[7] Photoluminescence properties of Eu^{2+} doped $M_2SiO_4:Eu^{2+}$ (M = Ca, Sr, Ba) and $M_1M_2SiO_4:Eu^{2+}$ ($M_{1,2}$ = Mg, Ca, Sr, Ba) also have been investigated in previous reports.[8] However, Ca_2SiO_4 has many kinds of crystal structures including α, α-H, α-L, β, γ, HP phases. Therefore, the different PL properties would be expected when doped with Eu^{2+} ions. Previously, we have prepared the novel $NaCa_{13/18}Mg_{5/18}PO_4:Eu^{2+}/Tb^{3+}/Mn^{2+}$ phosphors with trigonal system through the partial substitution of Ca by Mg from the familiar orthorhombic $NaCaPO_4$ phase.[9] This inspires us that the new crystal structure may be produced when part of certain elements in some familiar compounds are substituted by the same group ones. We notice that W. J. Park et al have ever tried to synthesize the $Ca_{2-x}Sr_xSiO_4:Eu^{2+}$ phosphors with the variation of x, but the phases vary therein and are different from that of α-$Ca_{1.65}Sr_{0.35}SiO_4$.[8h] Additionally, α-$Ca_{1.65}Sr_{0.35}SiO_4:Eu^{2+}$ prepared by Sakthivel Gandhia et al via solvo-thermal method presented two different phases. Therefore, the PL properties were not sure.[8i] Herein, we try to introduce partial Sr to replace Ca to obtain some different phases via the solid-state reaction synthesis in Ca_2SiO_4, fortunately, after some failures, the pure α-$Ca_{1.65}Sr_{0.35}SiO_4$ with orthorhombic structure and space group *P21cn* which is different from previously reported orthorhombic $CaSrSiO_4$ with *Pna21 or Pbnm*[10] appears in this process. In addition, the intense green emission excited under n-UV/UV light can be observed when introducing Eu^{2+} as an activator in this host. The phase purity (determined by Rietveld refinement), PL (involving temperature-dependent PL) properties and quantum yields of α-$Ca_{1.65}Sr_{0.35}SiO_4:Eu^{2+}$ were investigated in detail. The results suggest that it would be recognized as a promising phosphor for UV/n-UV w-LEDs.

2. Experiment section

2.1 Materials and preparation

The objective phosphors with the nominal chemical composition α-$Ca_{1.65}Sr_{0.35-x}SiO_4:xEu^{2+}$ (x = 0- 0.08 is the mole dopant concentration) were prepared via the high-temperature solid-state reaction method under reductive atmosphere. $CaCO_3$ (A.R.), $SrCO_3$ (A.R.), SiO_2 (A.R.) and Eu_2O_3 (99.99%), without any purity, were employed as the raw materials. In a typical process, the raw materials were weighed according to the given stoichiometric ratio and mixed thoroughly by grinding them in an agate mortar with appropriate ethanol addition, after which the mixture was shifted to the crucible and transformed to the tube furnace to calcine at 1200 °C for 8 h under $10\%H_2/90\%N_2$ atmosphere condition to generate the final samples following by reground for 1 min. After calcination, the samples were furnace-cooled to room temperature with constant reductive current, and then ground again into powders for the following measurements.

2.2 Characterization

D8 Focus diffractometer was utilized to measure the X-ray diffraction (XRD) patterns at a scanning rate of $10°min^{-1}$ in the 2θ range from 10° to 100° with graphite-monochromatized Cu K_α radiation (λ = 0.15405 nm). Infrared spectra were collected on a VERTEX 70 Fourier transform infrared (FT-IR) spectrometer (Bruker). The morphology of the sample was inspected using a scanning electron microscope (SEM, S-4800, Hitachi). The Hitachi F-7000 spectrophotometer equipped with a 150 W xenon lamp as the excitation source were used to conduct photoluminescence (PL) measurements, and the diffuse reflectance spectra were gained using a Hitachi U-4100 spectrophotometer with the reflection of black felt (reflection 3%) and white $BaSO_4$ (reflection 100%). The luminescence decay lifetimes were measured and obtained from a Lecroy Wave Runner 6100 Digital Osilloscope (1 GHz) using a tunable laser (pulse width = 4 ns, gate = 50 ns) as the excitation (Contimuum Sunlite OPO) source. PL quantum yields (QYs) of phosphors were obtained directly by the absolute PL quantum yield measurement system (C9920−02, Hamamatsu Photonics K. K., Japan). The solid-state NMR was measured with a conventional impulse spectrometer DSX advance (Bruker) operating with a resonance frequency of 500MHz for ^1H (B = 11.3 T). All the above measurements were performed at room temperature (RT). Moreover, the high resolution emission spectra and decay lifetimes at low temperature (77K), the temperature-dependent (298-523 K) PL spectra together with the emission spectrum at 10K were recorded on a fluorescence spectrophotometer equipped with a 450 W xenon lamp as the excitation source (Edinburgh Instruments FLSP-920) with a temperature controller.

3. Results and discussion

3.1 Crystal structure, Phase Identification and Purity.

The α-$Ca_{1.65}Sr_{0.35-x}SiO_4$ compound was first reported by Udagawa, S. et al in 1979, which has the orthorhombic structure similar to α-Ca_2SiO_4 with cell parameters a = 5.566 Å, b = 9.355 Å, c = 20.569 Å, Z = 12 and V = 1071.03 $Å^3$.[3,11] The detailed crystal structure of α-$Ca_{1.65}Sr_{0.35-x}SiO_4$ is presented in Fig. 1, which shows there are six kinds of Ca/Sr sites in one unit cell. The Ca1/Sr1, Ca2/Sr2, Ca3/Sr3 and Ca4/Sr4 are surrounded by 5, 6, 4, 8 oxygen atoms, respectively, while Ca5/Sr5 and Ca6/Sr6 are both coordinated by 7 oxygen atoms. Fig. 2 illustrates the experimental, calculated and differences of the Rietveld refinement conducted by the general structure analysis system (GSAS) method of powder XRD profile of representative α-$Ca_{1.65}Sr_{0.345}SiO_4:0.005Eu^{2+}$. The initial structure model of α-$Ca_{1.65}Sr_{0.35}SiO_4$ (ICSD 39100) crystallizing in orthorhombic system with space group *P21cn*

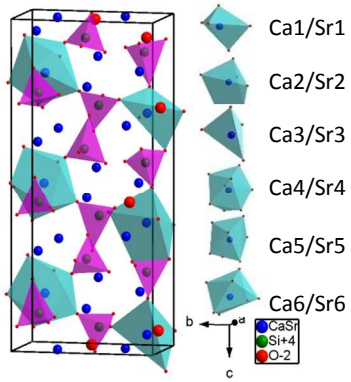

Fig. 1 Crystal structure of α-$Ca_{1.65}Sr_{0.35}SiO_4$ compound.

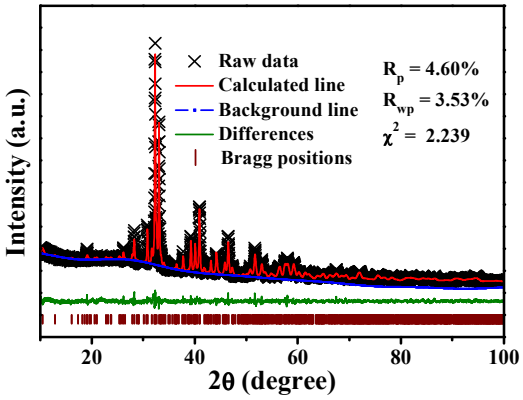

Fig. 2 Rietveld refinement of powder XRD profile of representative α-$Ca_{1.65}Sr_{0.345}SiO_4$:$0.005Eu^{2+}$.

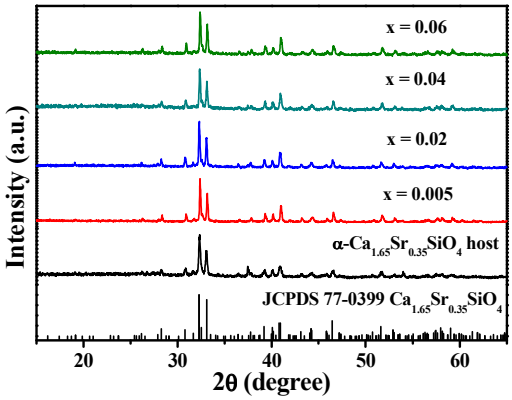

Fig. 3 Representative XRD patterns of α-$Ca_{1.65}Sr_{0.35-x}SiO_4$:$xEu^{2+}$ (x = 0-0.06) as well as the standard reference of α-$Ca_{1.65}Sr_{0.35}SiO_4$ compound (JCPDS card no.77-0399).

was used to refine the above sample. The reliability parameters of refinement are R_{wp} = 3.53%, R_p = 4.60%, χ^2 = 2.239, which can validate the phase purity of the as-prepared sample. The lattice constants a = 5.5475(1) Å, b = 9.3192(2) Å, c = 20.4457(5), Z = 12 and V = 1057.02(5) $Å^3$ also can be obtained. These detailed refined results are all presented in Table 1 below. Fig. 3 displays the representative XRD patterns of α-$Ca_{1.65}Sr_{0.35-x}SiO_4$:$xEu^{2+}$ (x = 0-0.06). All the diffraction peaks and profiles match well with those of the orthorhombic α-$Ca_{1.65}Sr_{0.35}SiO_4$ phase according to the standard reference of JCPDS no.77-0399 and no any traces of impurity phases are observed, indicating that Eu^{2+} can be well dissolved into this host and little change to crystal structure can be found. The similar ionic radii and same valence state between Eu^{2+} [r = 1.17 Å for coordination number (CN = 6), 1.20 Å for CN = 7, 1.25 Å for CN = 8] and Sr^{2+} (1.13 Å for CN = 6, 1.21 Å for CN = 7, 1.25 Å for CN = 8) ions suggest that Eu^{2+} would accommodate Sr^{2+} sites in this kind of host.

The FT-IR spectra of the α-$Ca_{1.65}Sr_{0.35}SiO_4$ host and Eu^{2+}-doped samples with different doping concentration together with the ^{29}Si MAS-NMR spectrum of the α-$Ca_{1.65}Sr_{0.35}SiO_4$ host have been presented in Fig. 4. We can observe that the profiles of FT-IR spectra of Eu^{2+}-doped samples are similar to α-$Ca_{1.65}Sr_{0.35-x}SiO_4$ host in Fig 4a, which indicates the accommodation of rare earth ions into this host has the little change to the structure of the α-$Ca_{1.65}Sr_{0.35}SiO_4$, consistent with the XRD analysis above. The two bond vibrations positions around 510 and 549 cm^{-1} correspond to the bending mode in plane of Si–O–Si of the SiO_4 tetrahedron, and the group of peaks around 828, 907, 984 cm^{-1} are assigned to the asymmetric Si–O stretching modes of the SiO_4 tetrahedron, which are in accordance with the data [400-600cm^{-1} refers to δ(SiO_4) and 900-1100 cm^{-1} refers to ν(SiO_4)] reported in previous literature.[12] The ^{29}Si MAS-NMR spectrum of the α-$Ca_{1.65}Sr_{0.35}SiO_4$ host shows an obvious resonance around 99.4 ppm in Fig. 4b, which further certifies the existence of SiO_4 tetrahedron in α-$Ca_{1.65}Sr_{0.35}SiO_4$ host. Another two absorption peaks of FT-IR spectra at about 1438 and 2916 cm^{-1} are attributed to the OH^- stretching vibrations mode deriving from the covered water on the surface of phosphors under air condition.

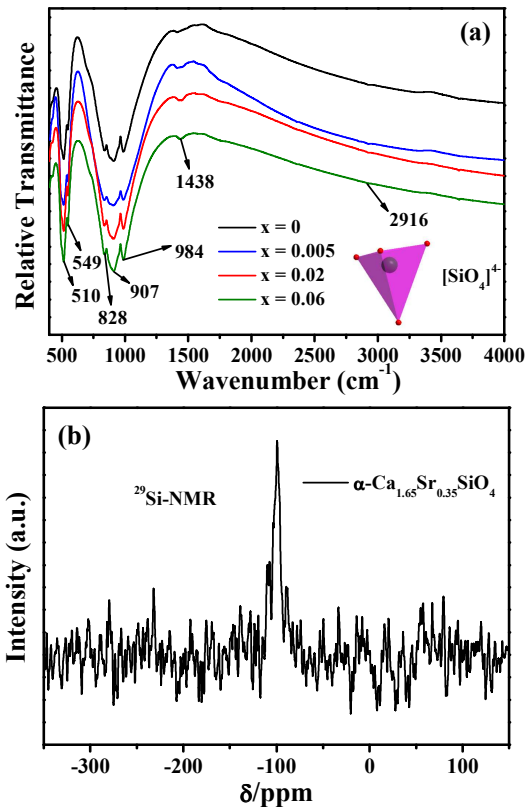

Fig. 4 FT-IR spectra of the α-$Ca_{1.65}Sr_{0.35-x}SiO_4$:$xEu^{2+}$ (x = 0-0.06) samples (a) and ^{29}Si MAS-NMR spectrum of α-$Ca_{1.65}Sr_{0.35}SiO_4$ host (b).

3.2 Diffuse refection and PL spectra of Eu^{2+} doped α-$Ca_{1.65}Sr_{0.35-x}SiO_4$ phosphor

The diffuse reflection spectra of the α-$Ca_{1.65}Sr_{0.35-x}SiO_4$:$xEu^{2+}$ (x = 0-0.06) phosphors are shown in Fig. 5. It is readily observed that there are apparent different profiles between α-$Ca_{1.65}Sr_{0.35}SiO_4$ host and Eu^{2+}-doped samples, which illustrate the Eu^{2+} can be as an effective activator and produce its characteristic excitation and emission spectra properties in this host. For α-$Ca_{1.65}Sr_{0.35}SiO_4$ host, it has two evident absorption bands corresponding to the wavelength ranges of 220-260 nm and 260-450 nm. However, the two different absorption bands ranging from 220-278 nm and 278-600 nm occur when Eu^{2+} ions are doped into the host, resulting from the Eu^{2+} 4f-5d

transition. In addition, the absorption extent of this series of samples increases constantly with the continuous increase of Eu^{2+} concentration, which further indicates that the absorptions in Eu^{2+} doped samples derive from Eu^{2+} ions transition. The Kubelka-Munk absorption coefficient (K/S) relationship was often used to determine the absorption edge approximately from the obtained diffuse reflectance spectrum:[13]

$$\frac{K}{S}=\frac{(1-R)^2}{2R} \quad (1)$$

where K refers to the absorption coefficient, S represents the scattering coefficient, and R is the reflectivity. According to the equation and reflection spectrum above, the optical band gap is evaluated approximately to be 4.21 eV (295 nm) for α-$Ca_{1.65}Sr_{0.35}SiO_4$, which is critical due to the valence to conduction band transitions of the α-$Ca_{1.65}Sr_{0.35}SiO_4$ host. Fig. 6a shows the PL emission (λ_{ex} = 350, 365 and 396 nm) and excitation (λ_{em} = 508 nm) spectra of the α-$Ca_{1.65}Sr_{0.34}SiO_4$:$0.01Eu^{2+}$ sample. The PL excitation spectrum monitored at 508 nm presents a wide band ranging from 220 to 475 nm, consistent with the diffuse reflection spectrum shown in Fig. 5, in which there are two obvious peaks around at 369 and 396 nm, corresponding to the $4f^7$- $4f^65d^1$ allowed transition of Eu^{2+} ion. However, the narrow peak at 396 nm may derive from Eu^{3+} excitation because the excitation peak of Eu^{3+} often occurs around 393 nm. Additionally, the broad extent of excitation spectrum would like to be interesting for application in n-UV w-LEDs, which is usually desired. The profiles of emission spectra with broad band ranging from 400 to 650 nm peaking at 508 nm originating from Eu^{2+} $4f^65d^1$ - $4f^7$ are similar except for the intensity under different excitation wavelengths of 350, 365 and 396 nm, which indicate the green emission colors are produced for α-$Ca_{1.65}Sr_{0.35-x}SiO_4$:$0.01Eu^{2+}$ sample under n-UV excitation and there is no sharp Eu^{3+} emission peak around about 613 nm observed, which indicates the Eu^{3+} can be reduced to Eu^{2+} completely. The full-width at half-maximum (FWHM) of the PL spectrum of is about 87 nm, which also indicates it covers a broad green-emitting area. The calculated Stokes shift between the excitation peak at 369 nm and emission peak at 508 nm is about 7415 cm^{-1}. Fig. 6c shows the emission spectra of 10 K and 298 K of α-$Ca_{1.65}Sr_{0.35-x}SiO_4$:$0.01Eu^{2+}$, from which we can see the FWHM of emission spectrum at 10 K is a little narrower than that at 298 K. This difference can be attributed to the vibration energy of the host lattice. The allowed $4f^65d^1 \rightarrow 4f^7$ transition can couple with the energy of the phonon vibrations in host, which can result in the widened emission band in the phosphor. At 10 K, the number of phonon vibrations is limited and the emission band is narrow. With the increase of temperature, the number of separate phonons increases and thus the emission band becomes widened. One can also find that the emission spectra at 10 and 298 K are asymmetric, which indicates that more than one Eu^{2+} emitting centers can be inferred in the host. Based on different coordination number around centered Sr which can generate different local crystal field environment and be substituted by Eu^{2+} ions, the familiar experiential equation proposed by Van Uitert has been used to analyze the present experimental result, which is shown below:[14]

$$E=Q\left[1-\left(\frac{V}{4}\right)^{\frac{1}{V}}10^{-\frac{n\times Ea\times r}{80}}\right] \quad (2)$$

Where E refers to the position of the d-band edge in energy for the rare-earth ion (cm^{-1}), Q corresponds to the position in energy for the lower d-band edge for the free ion (34 000 cm^{-1} for Eu^{2+}), V is the valence of the ''active'' cation, here V = 2 for Eu^{2+}. E_a is the electron affinity of the atoms that form anions (eV), which is different when Eu^{2+} is introduced into

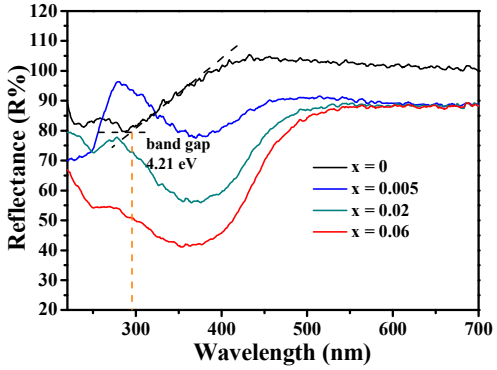

Fig. 5 Diffuse reflection spectra of the α-$Ca_{1.65}Sr_{0.35-x}SiO_4$:$xEu^{2+}$ (x = 0-0.06) samples.

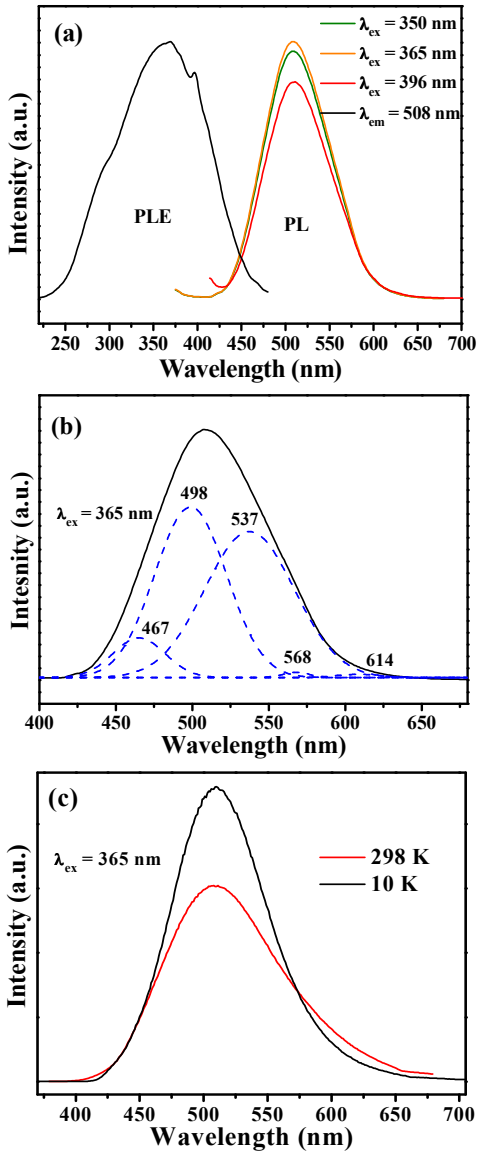

Fig. 6 (a) PL excitation and emission spectra of α-$Ca_{1.65}Sr_{0.34}SiO_4$:$0.01Eu^{2+}$. (b) Gaussian fitting into five emission bands from emission spectrum upon 365 nm

excitation. (c) Emission spectra at 10K and 298 K of α-$Ca_{1.65}Sr_{0.35-x}SiO_4$:0.01$Eu^{2+}$ upon 365 nm excitation.

different anion complexes with various coordination numbers. Moreover, *n* represents the number of anions in the immediate shell around the "active" cation, and *r* is the radius of the host cation (Sr^{2+}) replaced by the ''active'' cation (Eu^{2+}). According to this formula, it is easy to find that the value of *E* is proportional to the two parameters of *n* and *r*. Accordingly, we can infer that the emission peaks at 467, 498, 537, 568 and 614 nm obtained by Gaussian fitting of the emission spectrum excited at 365 nm in Fig. 6b correspond to Sr4 with 8-coordination, Sr5/Sr6 with 7-coordination, Sr2 with 6-coorination, Sr1 with 5-coordination and Sr3 with 4-coordination, respectively.

3.3 PL emissions and lifetimes of α-$Ca_{1.65}Sr_{0.345}SiO_4$:Eu^{2+} phosphors with various Eu^{2+} concentration

Fig. 7a shows the PL emission spectra of α-$Ca_{1.65}Sr_{0.35-x}SiO_4$:x$Eu^{2+}$ phosphors with various Eu^{2+} concentration x upon365 nm excitation, from which we can find the profiles of emission spectra are similar but a little different from each other. Moreover, the wavelength of emission peak increases from 504 nm to 522 nm under 365 nm excitation with the increase of Eu^{2+} concentration x from 0.001 to 0.08 in Fig. 7b, which may be caused by the occupations of different Sr^{2+} ions sites by Eu^{2+} ions with the increase of Eu^{2+} concentration. The obtained experimental optimal Eu^{2+} concentration x in α-$Ca_{1.65}Sr_{0.35-x}SiO_4$:x$Eu^{2+}$ is found to be 0.01, beyond which the PL emission intensity starts to decrease with increasing Eu^{2+} concentration attributed to the concentration quenching effect as illustrated in

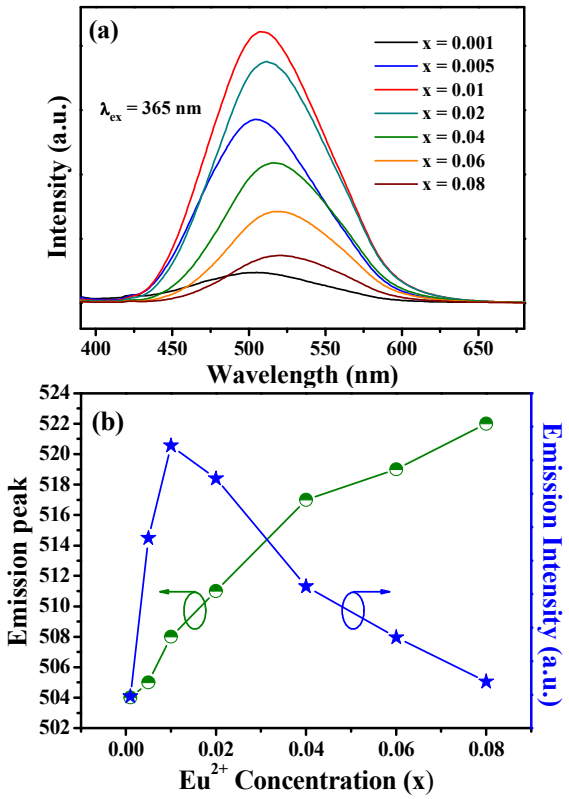

Fig. 7 (a) Variation of PL emission spectra of α-$Ca_{1.65}Sr_{0.35-x}SiO_4$:x$Eu^{2+}$ excited with 365 nm UV with different concentrations of Eu^{2+} ions. (b) Variations of emission peak and intensity with increasing Eu^{2+} concentration x in α-$Ca_{1.65}Sr_{0.35-x}SiO_4$:x$Eu^{2+}$ phosphors.

Fig. 8b which draws up the emission intensity of α-$Ca_{1.65}Sr_{0.35-x}SiO_4$:x$Eu^{2+}$ phosphors as a function of the Eu^{2+} content. The emission intensity increases with the increase of Eu^{2+} content and reaches a maximum at x = 0.01, then decreases with further Eu^{2+} concentration. It is accepted that concentration quenching occurs because of the energy transfer among Eu^{2+} ions, whose probability increases as the concentration of Eu^{2+} increases. In order to determine the energy transfer mechanism in α-$Ca_{1.65}Sr_{0.35}SiO_4$:Eu^{2+} samples, it is necessary to know the critical distance (R_c) between activators such as Eu^{2+} here. With the increasing of Eu^{2+} content, the distance between Eu^{2+} ions becomes shorter and shorter, thus the probability of energy migration increases. When the distance reaches small enough, the concentration quenching occurs and the energy migration is hindered. Therefore, the calculation of R_c has been pointed out by Blasse:[15]

$$R_c \approx 2\left[\frac{3V}{4\pi X_c N}\right]^{1/3} \quad (3)$$

where *V* corresponds to the volume of the unit cell, *N* is the number of host cations in the unit cell, and X_c is the critical concentration of dopant ions. For the α-$Ca_{1.65}Sr_{0.35}SiO_4$ host, *N* = 12, *V* = 1071.03 Å^3, and X_c is 1% for Eu^{2+}; Accordingly, the critical distance (R_c) was estimated to be about 25.74 Å.

In general, there are three mechanisms for non-radiate energy transfer including exchange interaction, radiation reabsorption, and electric multipolar interaction. The result obtained above indicates the little possibility of exchange interaction since the exchange interaction is predominant only for about 5 Å which is far less than 25.74 Å.[16] The mechanism of radiation reabsorption is only efficacious when the fluorescence and absorption spectra are widely overlapping, which also does not intend to occur in this case. Consequently, we can conclude the energy transfer mechanism between Eu^{2+} ions is only electric multipolar interaction. According to the formula proposed by Dexter and Van Uitert, which can be expressed as follow:[17]

$$\frac{I}{x} = \left[1+\beta(x)^{\theta/3}\right]^{-1} \quad (4)$$

where *I* represents the emission intensity, *x* is the activator ion concentration, and *β* is a constant for the given matrix under the identical excitation conditions. The type of energy transfer mechanism of electric multipolar interaction can be estimated by analyzing the constant *θ* from this formula. The value of *θ* is 6, 8, 10, corresponding to electric dipole-dipole, dipole-

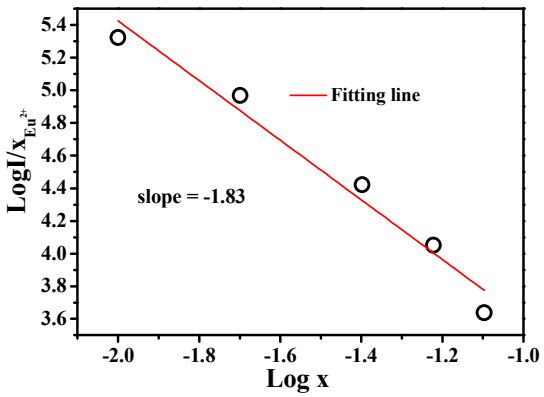

Fig. 8 Linear fitting of log(x) versus log(I/x) in various α-$Ca_{1.65}Sr_{0.35-x}SiO_4$:x$Eu^{2+}$ phosphors beyond the concentration quenching (x>0.01).

quadrupole or quadrupole-quadrupole interactions, respectively. The curve of log(I/x) versus log(x) in α-$Ca_{1.65}Sr_{0.345}SiO_4$:Eu^{2+} phosphors beyond the quenching content of Eu^{2+} was plotted in Fig. 8 to determine the value of θ, which shows a fitted straight line with a slope equal to -1.83 = -θ/3, as a consequence, the θ = 5.49 is approximately as 6, indicating the dipole-dipole interaction dominates the energy transfer mechanism between Eu^{2+} in α-$Ca_{1.65}Sr_{0.345}SiO_4$:Eu^{2+} phosphors.

As an important parameter for phosphors applied in the field of display and lighting, the decay lifetimes of them were used to analyze the concentration quenching in detail. Fig. 9 depicts the decay curves of α-$Ca_{1.65}Sr_{0.35-x}SiO_4$:x$Eu^{2+}$ (x = 0.001, 0.01, 0.02, 0.04 and 0.08) samples excited at 390 nm and detected at 508 nm, whose data are plotted as a semi-logarithmic plot. The decay curves gradually deviates from the linear with increasing Eu^{2+} concentration. Therefore, the decay lifetimes can be approximately evaluated using the following equation:[18]

$$\tau = \int_0^\infty I(t)dt \quad (5)$$

where τ refers to calculated lifetime value, and *I(t)* is the normalized intensity of emission spectra. According to above formula and decay curves, the values of decay lifetimes were determined to be 0.71, 0.67, 0.60, 0.53 and 0.37 μs for α-$Ca_{1.65}Sr_{0.35-x}SiO_4$:x$Eu^{2+}$ corresponding to x = 0.001, 0.01, 0.02, 0.04 and 0.08, respectively, which show the lifetime decreases with the increase of Eu^{2+} content, as presented in previous reports.[5c,19] The measured lifetimes also can be related to the total relaxation rate by:[20]

$$\frac{1}{\tau} = \frac{1}{\tau_0} + A_{nr} + P_t \quad (6)$$

where τ_0 is the radiative lifetime, A_{nr} is the nonradiative rate attributed to multiphonon relaxation, and P_t is the energy transfer rate between Eu^{2+} ions. With the increase of Eu^{2+} concentration, the distance between Eu^{2+} ions decreases. Therefore, both the probability of energy transfer to luminescent killer sites between Eu^{2+}-Eu^{2+} ions groups and the energy transfer rate increases. As a consequence, the lifetimes decrease with increasing Eu^{2+} content. Additionally, we measured the high resolution emission spectra and decay times at low temperature (77K) for three representative samples α-$Ca_{1.65}Sr_{0.35-x}SiO_4$:x$Eu^{2+}$ (x = 0.01, 0.02 and 0.04), which are presented in Fig. 10. The emission spectra upon 365 nm excitation are asymmetric and the profiles are similar to each other in Fig. 10a. And the emission intensity decreases with increasing Eu^{2+} dopant concentration, which is in accordance with that at room temperature. The decay times are calculated to be 729.1, 664 and 620.1 ns corresponding to x = 0.01, 0.02 and 0.04 according to the equation (5) and decay curves in Fig. 10b, which are bigger than those of corresponding ones at room temperature, respectively, originating from the decrease of lattice vibration at low temperature.

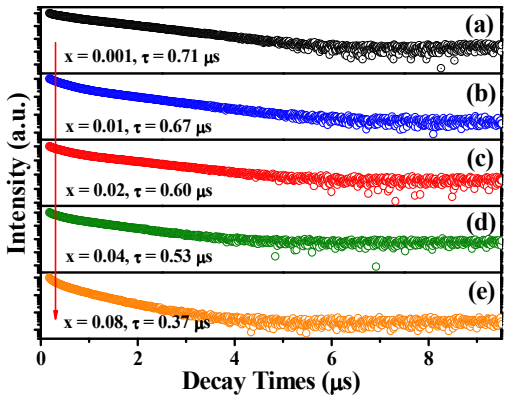

Fig. 9 Variation of fluorescent decay times excited at 390 nm and monitored at 508 nm in various α-$Ca_{1.65}Sr_{0.35-x}SiO_4$:x$Eu^{2+}$ [(a) x = 0.001, (b) x = 0.01, (c) x = 0.02, (d), x = 0.04 and (e) x = 0.08] phosphors.

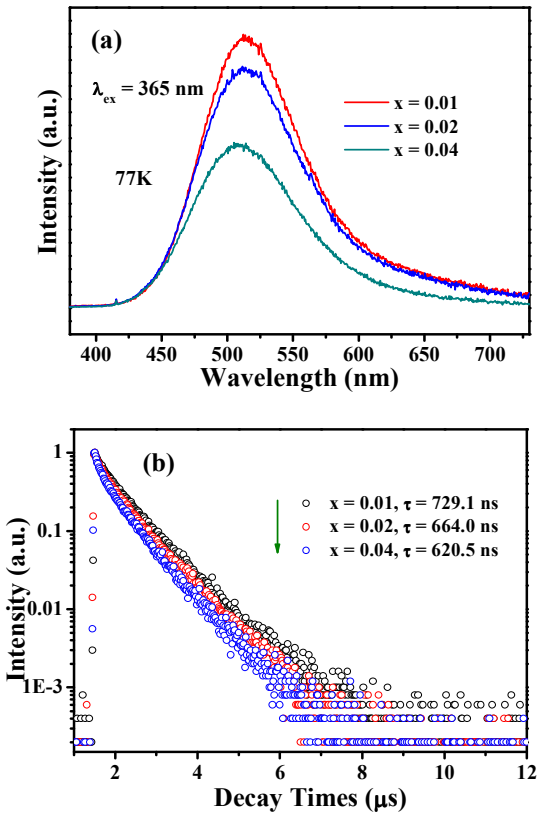

Fig. 10 (a) PL emission spectra of representative α-$Ca_{1.65}Sr_{0.35-x}SiO_4$:x$Eu^{2+}$ excited at 365 nm (x = 0.01, 0.02 and 0.04) at 77K. (b) Decay curves of corresponding samples monitored at 508 nm and excited at 390 nm.

3.4 SEM image, CIE chromaticity coordinates and quantum yields

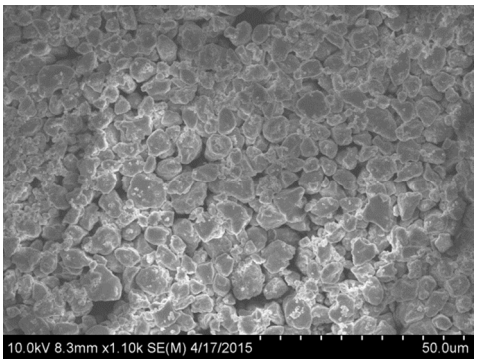

Fig. 11 SEM image of the selected α-$Ca_{1.65}Sr_{0.34}SiO_4$:0.01Eu^{2+} sample.

Table 1 The variation of CIE chromaticity coordinates (x, y) and quantum yields (QYs) for α-$Ca_{1.65}Sr_{0.35-x}SiO_4$:x$Eu^{2+}$ phosphors excited at 365 nm UV radiation

Sample No.	Eu^{2+} concentration (x)	CIE coordinates (x, y)	QY(%)
1	0.001	(0.197, 0.395)	24
2	0.005	(0.192, 0.447)	69
3	0.01	(0.205, 0.478)	49
4	0.02	(0.214, 0.501)	34
5	0.04	(0.229, 0.531)	27
6	0.06	(0.237, 0.546)	23
7	0.08	(0.242, 0.547)	16

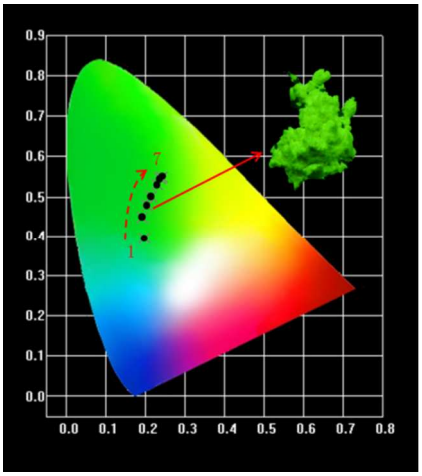

Fig. 12 CIE chromaticity coordinates diagram of the as-prepared samples α-$Ca_{1.65}Sr_{0.35-x}SiO_4$:x$Eu^{2+}$ with increasing Eu^{2+} concentration x and the selected digital photo of α-$Ca_{1.65}Sr_{0.34}SiO_4$:0.01Eu^{2+} under 365 nm UV lamp excitation.

Fig. 11 shows the microstructure and morphology of the representative α-$Ca_{1.65}Sr_{0.34}SiO_4$:0.01Eu^{2+} sample, which were determined using SEM. It is observed that the particles have been dispersed after polishing and ultrasonic treating, therefore, we estimate approximately the size distribution with diameters of particles between 3 and 15 μm from the section of particles without aggregation signed with red circle in photograph, which may be very helpful in practical terms in the fabrication of white LEDs devices. As two important parameters, CIE chromaticity coordinates and quantum yields of α-$Ca_{1.65}Sr_{0.35-x}SiO_4$:x$Eu^{2+}$ phosphors have also been investigated and measured under 365 nm excitation. We can see the CIE chromaticity coordinate gradually varies from (0.197, 0.395) to (0.242, 0.547) corresponding to x = 0.001 and 0.08, respectively, which indicates the value gradually shifts from green region to the border of green and yellow area with increasing Eu^{2+} concentration in Fig. 12 and is in accordance with the red shift of corresponding emission spectra. Selected inset is the digital luminescent sample of α-$Ca_{1.65}Sr_{0.34}SiO_4$:0.01Eu^{2+} upon 365 nm UV lamp excitation, displaying bright green emission color. The measured values of quantum yields of as-prepared samples are listed in Table 1. The maximum quantum yield in as-prepared samples can reach 69% for α-$Ca_{1.65}Sr_{0.345}SiO_4$:0.005Eu^{2+} excited at 365 nm, which can be further improved by controlling the particle morphology, size, and crystalline defects via optimizing the synthesis method and process, as well as chemical composition.

3.5 Temperature-dependent PL properties

Thermal stability is a crucial technology parameter for a phosphor that should be indispensable to be taken into account when applied in solid-state lighting, especially in high-power LEDs. It should keep stable emission efficiency at the temperature of above 150 °C for a long period of time.[21] In order to assess the influence of temperature on luminescence and determine the activation energy for thermal quenching, the temperature-dependent PL emission spectra (25 °C -250 °C) for represented α-$Ca_{1.65}Sr_{0.34}SiO_4$:0.01Eu^{2+} sample under 370 nm excitation was measured and plotted in Fig. 13a. As is depicted, the relative PL emission intensity gradually decreases with constantly increasing temperature from room temperature (25 °C) to 250 °C. Generally, the decrease of emission intensity is ascribed to the thermal quenching of emission intensity via phonon interaction, in which the excited luminescence center is thermally activated through the crossing point between the ground and the excited states. In addition, the integrated intensity at 150 °C drops to about 66% of the original value at room temperature, which is higher than that (about 49%) of commercial green-emitting $(Ba,Sr)_2SiO_4$ phosphor, as is shown in the inset of Fig. 13a. This indicates the as-prepared samples can present good thermal stability properties. Simultaneously, we can find the emission peak of α-$Ca_{1.65}Sr_{0.34}SiO_4$:0.01Eu^{2+} sample gradually shifts to short wavelength with the increase of operated temperature, which can be ascribed to the thermally

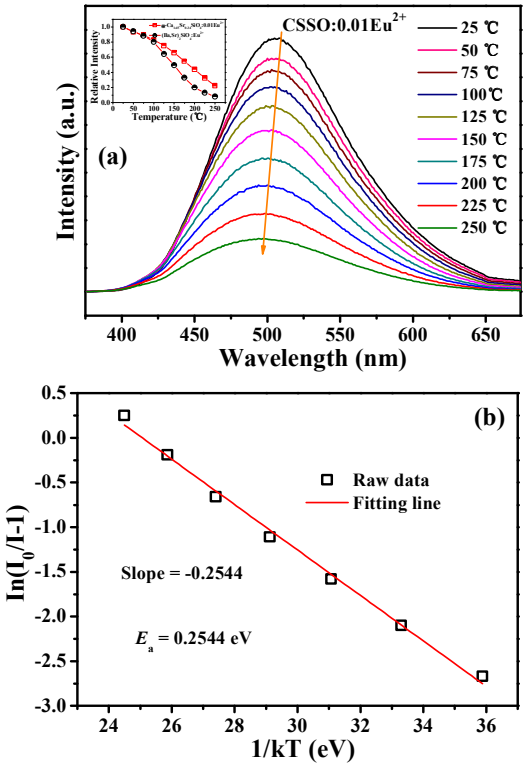

Fig. 13 (a) Temperature-dependent PL spectra of α-$Ca_{1.65}Sr_{0.34}SiO_4$:0.01Eu^{2+} phosphor; inset shows the integrated intensity vs. temperature (λ_{ex} = 365 nm). (b) The relationship of

$In(I_0/I-1)$ versus 1/kT activation energy graph for thermal quenching for α-$Ca_{1.65}Sr_{0.34}SiO_4$:0.01Eu^{2+} sample.
active phonon-assisted excitation from the excited states of the lower-energy emission band to the higher-energy emission band in the excited states of Eu^{2+}.[22] In order to calculate the activation energy (E_a) for thermal quenching and better understand the thermal quenching phenomenon, the relationship of $In(I_0/I-1)$ versus $1/kT$ activation energy graph for thermal quenching of α-$Ca_{1.65}Sr_{0.34}SiO_4$:0.01Eu^{2+} sample was plotted in Fig. 13b according to the following formula given by Arrhenius:[23]

$$In\left(\frac{I_0}{I}\right) = InA - \frac{E_a}{kT} \quad (7)$$

Herein, I_0 represents the original emission intensity at room temperature 25 °C, I is the emission intensity at different objective temperature. A is a constant for a certain host, E_a refers to the activation energy of thermal quenching (which is the energy required to raise the electron from the relaxed excited level into the host lattice conduction band), and k is the Boltzmann constant (8.626×10^{-5} eV). Therefore, the E_a was calculated to be 0.2544 eV from the slope of the fitting straight line.

4. Conclusions

In summary, we have studied a novel green-emitting phosphor α-$Ca_{1.65}Sr_{0.35}SiO_4$:Eu^{2+} in detail which is synthesized via the high-temperature solid-state reaction route. The phase category and their purity are examined by the XRD pattern and Rietveld refinement. The analysis of crystallographic occupancy was used to identify the emission centers of Eu^{2+} from the structure. The as-synthesized α-$Ca_{1.65}Sr_{0.35}SiO_4$:0.01Eu^{2+} shows wide and strong absorption in the UV and n-UV areas and the primary excitation range of 200-475 nm which is suitable for UV or n-UV pumped LED chips. Upon 365 nm excitation, the phosphors present intense and bright green emissions, however, the emission peak shifts to longer wavelength with increasing Eu^{2+} content. The energy transfer mechanism between Eu^{2+} ions is determined to be dipole-dipole interaction via the concentration quenching method. The SEM image, CIE coordinates and quantum yields have also been investigated in detail. The maximum quantum yield obtained was 69% for α-$Ca_{1.65}Sr_{0.345}SiO_4$:0.005Eu^{2+} sample upon 365 nm excitation. What's more, the thermal stability of representative α-$Ca_{1.65}Sr_{0.35}SiO_4$:0.01Eu^{2+} can be comparable to the commercial green-emitting $(Ba,Sr)_2SiO_4$ phosphor. These above results indicate the potential application as a green component in tricolor UV or n-UV pumped w-LEDs.

Acknowledgments

This project is financially supported by the National Natural Science Foundation of China (NSFC Grants 51472234, 51172227, 91433110), National Basic Research Program of China (Grants 2014CB643803), and Joint Funds of the National Natural Science Foundation of China (Grant U13012038).

References

1 (a) E. F. Schubert and J. K. Kim, *Science*, 2005, **308**, 1274; (b) J. Zhong, W. Zhao, L. Lan, J. Wang, J. Chen and N. Wang, *J. Alloys Compd*., 2014, **592**, 213; (c) C.-H. Huang, T.-S. Chan, W.-R. Liu, D.-Y. Wang, Y.-C. Chiu, Y.-T. Yeh and T.-M. Chen, *J. Mater. Chem*., 2012, **22**, 20210; (d) Y.-C. Chiu, C.-H. Huang, T.-J. Lee, W.-R. Liu, Y.-T. Yeh, S.-M. Jang and R.-S. Liu, *Opt. Exp*., 2011, **19**, A331.
2 (a) Z. Xia, Y. Zhang, M. S. Molokeev and V. V. Atuchin, *J. Phys. Chem. C*, 2013, **117**, 20847; (b) J. Sun, G. Shen, X. Wang, D. Shen and J. Sun, *Mater. Res. Bull*., 2013, **48**, 3695; (c) P. Shi, Z. Xia, M. S. Molokeevc and V. V. Atuchind, *Dalton Trans*., 2014 , **43**, 9669.
3 (a) J. S. Kim, P. E. Jeon, J. C. Choi and H. L. Park, *Appl. Phys. Lett*., 2004, **84**, 2931; (b) S.-P. Lee, C.-H. Huang and T.-M. Chen, *J. Mater. Chem. C*, 2014, **2**, 8925; (c) Y. Song, G. Jia, M. Yang, Y. Huang, H. You and H. Zhang, *Appl. Phys. Lett*., 2009, **94**, 091902.
4 (a) J. Lü, Y. Huang, L. Shi and H. J. Seo, *Appl. Phys. A*, 2010, **99**, 859; (b) P. Dorenbos, *J. Lumin*., 2003, **104**, 239.
5 (a) Z. Xia, J. Zhou and Z. Mao, *J. Mater. Chem. C*, 2013, **1**, 5917; (b) J. S. Kim, H. J. Song, H.-S. Roh, D. K. Yim, J. H. Noh and K. S. Hong, *Mater. Lett*., 2012, **79**, 112; (c) G. Lee, J. Y. Han, W. B. Im, S. H. Cheong and D. Y. Jeon, *Inorg. Chem*., 2012, **51**, 10688; (d) C.-W. Yeh, W.-T. Chen, R.-S. Liu, S.-F. Hu, H.-S. Sheu, J.-M. Chen and H. T. Hintzen, *J. Am. Chem. Soc*., 2012, **134**, 14108; (e) W. B. Park, S. P. Singh, C. Yoon and K.-S. Sohn, *J. Mater. Chem. C*, 2013, **1**, 1832.
6 (a) B. Yuan, Y. Huang, Y. M. Yu and H. J. Seo, *Ceram. Inter*., 2012, **38**, 2219; (b) Y. Song, Q. Liu, X. Zhang, X. Fang and T. Cui, *Mater. Res. Bull*., 2013, **48**, 3687; (c) J. Wang, Y. Huang, X. Wang, L. Qin and H. J. Seo, *Mater. Res. Bull*., 2014, **55**, 126.
7 (a) J. S. Kim, K. T. Lim, Y. S. Jeong, P. E. Jeon, J C. Choi and H. L. Park, *Solid State Comm*., 2005, **135**, 21; (b) S. H. Lee, J. H. Park, S. M. Son and J. S. Kim, *Appl. Phys. Lett*., 2006, **89**, 221916; (c) W. J. Parka, M. K. Junga, S. M. Kanga, T. Masakia and D.H. Yoon, *J. Phys. Chem. Solids*, 2008, **69**, 1505; (d) Q. Fei, C. Chang and D. Mao, *J. Alloys Compd*., 2005, **390**, 133.
8 (a) C. Guo, Y. Xu, F. Lv and X. Ding, *J. Alloys Compd*., 2010, **497**, L21; (b) J. H. Lee and Y. J. Kim, *Mater. Sci. Eng. B*, 2008, **146**, 99; (c) Z. Pan, H. He, R. Fu, S. Agathopoulos and X. Song, *J. Lumin*., 2009, **129**, 1105; (d) N.-S. Choi, K.-W. Park, B.-W. Park, X.-M. Zhang, J.-S. Kim, P. Kung and S. M. Kim, *J. Lumin*., 2010, **130**, 560; (e) Y. Y. Luo, D. S. Jo, K. Senthil, S. Tezuka, M. Kakihana, K. Toda, T. Masaki and D. H. Yoon, *J. Solid State Chem*., 2012, **189**, 68; (f) J. Barzowska, K. Szczodrowski, M. Krosnicki, B. Kuklinski and M. Grinberg, *Opt. Mater*., 2012, **34**, 2095; (g) J. S. Lee and Y. J. Kim, *Ceram. Inter*., 2013, **39**, S555; (h) H.-J. Woo, S. Gandhi, B.-J. Kwon, D.-S. Shin, S. S. Yi, J. H. Jeong and K. Jang, *Ceram. Inter*., 2015, **41**, 5547; (i) S. Gandhi, K. Thandavan, B.-J. Kwon, H.-J. Woo, K. Jang and D.-S. Shin, *Ceram. Inter*., 2014, **40**, 5245; (j) H. He, R. Fu, X. Song, D. Wang and J. Chen, *J. Lumin*., 2008, **128**, 489.
9 K. Li, J. Fan, X. Mi, Y. Zhang, H. Lian, M. Shang and J. Lin, *Inorg. Chem*., 2014, **53**, 12141.
10 (a) S. Tezuka, Y. Sato, T. Komukai, Y. Takatsuka, H. Kato and M. Kakihana, *Appl. Phys. Express*, 2013, **6**, 072101; (b) B.-J. Kwon, S. Gandhi, H.-J. Woo, K. Jang, D.-S. Shin, K. Kim and S. Jeong, *J. Kor. Phys. Soc*., 2014, **64**, 1721.
11 S. Udagawa, K. Urabe, T. Yano, K. Takada and M. Natsume, *Semento Hijutsu Nempo*, 1979, **33**, 35.
12 (a) G. Buhler, A. Zharkouskaya and C. Feldmann, *Solid State Sci*., 2008, **10**, 461; (b) D. V. Sunitha, H. Nagabhushana, F. Singh, S. C. Sharma, N. Dhananjaya, B. M. Nagabhushana and R. P. S. Chakradhare, *Spectrochimica Acta Part A*, 2012, **90**, 18.
13 (a) N. Yamashita, *J. Phys. Soc. Jpn*., 1973, **35**, 1089; (b) X.

Chen, Z. Xia and Q. Liu, *Dalton Trans*., 2014, **43**, 13370.
14 (a) L. G. van Uitert, *J. Lumin*., 1984, **29**, 1; (b) K. Li, D. Geng, M. Shang, Y. Zhang, H. Lian and J. Lin, *J. Phys. Chem. C*, 2014, **118**, 11026.
15 (a) G. Blasse, *J. Solid State Chem*., 1986, **62**, 207; (b) L. Wu, B. Wang, Y. Zhang, L. Li, H. R. Wang, H. Yi, Y. F. Kong and J. J. Xua, *Dalton Trans*., 2014, **43**, 13845.
16 (a) D. L. Dexter, *J. Chem. Phys*., 1969, **21**, 131; (b) W. R. Liu, C. H. Huang, C. P. Wu, Y. C. Chiu, Y. T. Yeh and T. M. Chen, *J. Mater. Chem*., 2011, **21**, 6869.
17 (a) L. G. Van Uitert, *J. Electrochem. Soc*., 1967, **114**, 1048; (b) D. L. Dexter, *J. Chem. Phys*., 1953, **21(5)**, 836.
18 (a) W. Lu, Y. Jia, W. Lv, Q. Zhao and H. You, *New J. Chem*., 2014, **38**, 2884; (b) D. Hou, C. Liu, X. Ding, X. Kuang, H. Liang, S. Sun, Y. Huang and Y. Tao, *J. Mater. Chem. C*, 2013, **1**, 493.
19 (a) Z. Xia, J. Zhuang, L. Liao, H. Liu, Y. Luo and P. Du, *J. Electroche. Soc*., 2011, **158**, J359; (b) K. Geng, Z. Xia and M. S. Molokeev, *Dalton Trans*., 2014, **43**, 14092.
20 D. Y. Wang, C. H. Huang, Y. C. Wu and T. M. Chen, *J. Mater. Chem*., 2011, **21**, 10818.
21 (a) D. Geng, M. Shang, Y. Zhang, H. Lian and J. Lin, *Inorg. Chem*., 2013, **52**, 13708; (b) C. W. Yeh, W. T. Chen, R. S. Liu, S. F. Hu, H. S. Sheu, J. M. Chen and H. T. Hintzen, *J. Am. Chem. Soc*., 2012, **134**, 14108.
22 (a) D. Hsu and J. L. Skinner, *J. Chem. Phys*., 1984, **81**, 5471; (b) M. Que, Z. Ci, Y. Wang, G. Zhu, S. Xin, Y. Shi and Q. Wang, *CrystEngComm*., 2013, **15**, 6389.
23 (a) R. J. Xie and N. Hirosaki, *Appl. Phys. Lett*., 2007, **90**, 191101; (b) W. R. Liu, C. H. Huang, C. W. Yeh, J. C. Tsai, Y. C. Chiu, Y. T. Yeh and R. S. Liu, *Inorg. Chem*., 2012, **51**, 9636; (c) Z. Lian, J. Sun, L. Zhang, D. Shen, G. Shen, X. Wang and Q. Yan, *RSC Adv*., 2013, **3**, 16534.

Graphic Abstract

A series of Eu^{2+}-doped α-$Ca_{1.65}Sr_{0.35}SiO_4$ phosphors synthesized via the high-temperature solid-state reaction method can emit intense green light under UV/n-UV excitation, which shows the potential application in UV/n-UV-pumped white-light-emitting diodes.